Published in final edited form as:
J Neuropathol Exp Neurol. 2009 October ; 68(10): 1147–1154. doi:10.1097/NEN.0b013e3181b9d75f.

Reduced Ratio of Afferent to Total Vascular Density in Mesial Temporal Sclerosis

Ryan T. Mott, MD[1], **Clara R. Thore, PhD**[2], **Dixon M. Moody, MD**[2], **Steven S. Glazier, MD**[3], **Thomas L. Ellis, MD**[4], and **William R. Brown, PhD**[1,2]

[1]Wake Forest University School of Medicine, Department of Pathology, Winston-Salem, North Carolina

[2]Wake Forest University School of Medicine, Department of Radiology, Winston-Salem, North Carolina

[3]Medical University of South Carolina, Department of Neuroscience, Division of Neurosurgery, Charleston, South Carolina

[4]Wake Forest University School of Medicine, Department of Neurosurgery, Winston-Salem, North Carolina

Abstract

Mesial temporal sclerosis (MTS) is the most common cause of drug-resistant temporal lobe epilepsy in adults. Despite nearly 2 centuries since the first reports of MTS, relatively little is known about its etiology and pathogenesis. Increasing attention has been directed toward the potential role of vascular abnormalities in MTS. We evaluated the hippocampal microvasculature in 9 MTS cases and 3 non-MTS controls using celloidin tissue sections and markers for total (collagen type IV) and afferent (enzymatic alkaline phosphatase) vessels. Tissue sections were assessed by light microscopy and quantified by threshold analysis of digital images and stereological analysis using the Space Balls probe. Although consistent alterations in the total microvascular density were not found there was a significant reduction in the density of afferent vessels using both methodologies; these reductions were in areas CA2 and CA3 by image threshold analysis and in area CA3 using stereological measures of the ratio of afferent to total vessels. Increased numbers of string vessels (i.e. remnants of regressing vasculature) were also observed in Ammon's horn, suggesting vascular degeneration in the MTS hippocampus. These findings may help further our understanding of the pathophysiology of MTS.

Keywords

Afferent vessels; Alkaline phosphatase; Blood-brain barrier; Collagen type IV; Mesial temporal sclerosis; String vessels; Temporal lobe epilepsy

Introduction

Mesial temporal sclerosis (MTS) is the most common cause of drug-resistant temporal lobe epilepsy in adults (1–4). Patients typically present in the second decade with complex partial seizures. Magnetic resonance (MR) imaging studies may show unilateral or bilateral disease

Send correspondence and reprint requests to: Clara R. Thore, PhD, Microvascular Research Lab, Dept. of Diagnostic Radiology, Wake Forest Univ. Sch. Med., Medical Center Blvd., Winston-Salem, NC 27157. Ph: (336) 784-5341; Fax: (336) 716-4407. cthore@wfubmc.edu.

with the characteristic features of a high signal intensity in the hippocampus on T2-weighted images, hippocampal atrophy and enlargement of the temporal horn of the lateral ventricle (5), MTS is characterized pathologically by neuronal loss and gliosis in Ammon's horn with accentuation in areas CA1 and CA4 (6). In severe cases, the alterations may extend into areas CA2 and CA3 (7). Granule cell dispersion in the dentate gyrus is also a recognized component of MTS pathology (8).

MTS was initially described in 1825 by Bouchet and Cazauvieil (9). Decades later, Sommer provided a detailed pathologic description of MTS, emphasizing the loss of pyramidal neurons in Ammon's horn (6). Soon after, these observations were confirmed in a large series by Bratz (10). Despite nearly 2 centuries of investigation, relatively little is known about the etiology and pathogenesis of MTS. Several studies have found an association with prolonged febrile seizures during infancy (1,11–13), but this association is present in only a minority of cases; this has led many to speculate that a more fundamental mechanism may be involved. Interestingly, in their original descriptions from the 19th century, Sommer and Bratz drew attention to vascular alterations in the sclerotic regions of the hippocampus, including what was described as proliferation of the microvasculature (10). Despite these initial observations, the potential role of vascular abnormalities in MTS has until recently been largely overlooked. Rigau et al described an increase in vascular density in all hippocampal areas from patients with temporal lobe epilepsy, regardless of etiology (14). They also described extravasation of IgG around hippocampal vessels, suggesting a disruption of the blood-brain barrier (BBB). Van Vliet et al also found evidence of BBB leakage in the form of extravasated albumin in temporal lobe epilepsy specimens (15). Hildebrandt et al recently described pathologic alterations of afferent vessels (i.e. arterioles and capillaries) in the white matter of pediatric patients with intractable focal epilepsies, including splitting of basement membranes and enlargement of perivascular spaces (16). Animal models have also shown microvascular alterations in the setting of chronic seizures. For example, Marcon et al used a status epilepticus model of epileptogenesis in developing rats and found an increase in the density of hippocampal microvessels in a subset of rats with chronic seizures (17). These changes were not observed in all of the rats with chronic seizures and were conspicuously absent in the rats exposed to the epileptogenic drug at an early postnatal period. Hellsten et al also found a significant increase in endothelial cell proliferation and total vessel length in the molecular layer of the dentate gyrus using a rat model of electroconvulsive therapy (18).

These recent studies have emphasized the potential role of microvascular pathology in MTS. To investigate this issue further, we examined temporal lobe tissues from MTS and control patients using techniques that allow for visualization of the 3-dimensional vascular architecture within the hippocampus. Herein, we describe novel pathologic alterations in the MTS hippocampal microvasculature.

Materials and Methods

Temporal lobe tissues were obtained from patients undergoing temporal lobectomies for medically intractable seizures. Each case in the MTS group was pathologically confirmed as MTS with no additional neuropathologic abnormalities. Using these criteria, a total of 9 MTS cases were examined in 2 different analyses. All patients gave their consent for these studies based on the guidelines of the Internal Review Board (IRB) at Wake Forest University School of Medicine. Temporal lobe tissues from 3 autopsy brains were used as controls. The IRB at Wake Forest University School of Medicine does not require informed consent from next of kin for the investigation of autopsy material. To qualify as controls, the brains had to be free of significant pathologic changes such as trauma, infarcts, vascular disease, brain tumors, degenerative disease or infection; no medical examiner cases were used.

Unfixed, fresh tissues were taken during the time of surgery or at the time of autopsy and were processed as previously described (19). Briefly, the brain slices were fixed for 48 hours in several changes of 70% ethanol at 4°C prior to dehydration and embedded in celloidin (10% parlodian in ethanol:ether; VWR Scientific, West Chester, PA). Specimens were then serially sectioned on a base sledge microtome at 100 μm for threshold analysis evaluations and at 66 μm for stereological evaluations. Only cases with sections oriented in the coronal plane and with a clearly identifiable hippocampal structure were analyzed.

Hippocampal sections were labeled with alkaline phosphatase (AP) histochemistry and visualized by lead deposition. In AP-stained tissue sections counterstained with cresyl violet acetate and light green, dense, uniform AP labeling is evident in the endothelial cells of capillaries and smaller arterioles; post-capillary venules and small veins are AP-negative and only take up the counterstain. Therefore, efferent vessels are easily differentiated in thick sections even at lower magnification (20–23). Total blood vessels were labeled by staining the sections with mouse monoclonal antibodies specific to human amniotic type IV collagen (MAB1910, Chemicon, Inc., Temecula, CA) diluted 1:5,000 in 2% normal goat serum. Floating sections were incubated overnight in the primary antibody, followed by incubation in biotinylated anti-mouse IgG (KPL, Inc. Gaithersburg, MD). Antibodies were visualized using streptavidin horseradish peroxidase and diaminobenzidine/H2O2 (DAB kit; Vector Labs, Burlingame, CA) following the manufacturer's instructions. Sections were also stained for structure using Gill's hematoxylin and eosin (Fisher Scientific, Pittsburgh, PA).

Quantification of Microvascular Densities

Microvascular densities were evaluated on the collagen type IV- and AP-labeled tissue sections for examination of total microvessels and afferent vessels, respectively. The anatomic subdivisions of the hippocampus were delineated by a neuropathologist (R.T.M.). The microvascular densities were compared among the hippocampal subdivisions both semiquantitatively and quantitatively using 2 different methods of computerized image morphometry: 1) threshold analysis of saved digital images and 2) real-time stereological analysis of vascular length/volume using the Space Balls probe in a 3-dimensional region of interest.

Threshold Analysis of Afferent Vessel Density (Area Fraction)

Preliminary studies of vessel density in hippocampal areas from 4 MTS patients and 3 non-MTS controls were done by threshold analysis of digital images, as previously described (19, 24). Selected areas were visualized at 20× magnification with a Nikon Eclipse E600 microscope (Nikon Instruments, Inc., Melville, NY) and images were captured digitally with a 2.2 MP SPOT Flex digital camera (Diagnostic Instruments, Inc., Sterling Heights, MI). Color images were 2048 × 2048 pixels and encompassed a 2.21 mm^2 area on the section. Hippocampal areas (i.e. subiculum, CA1, CA2, CA3, CA4, and dentate gyrus) were outlined on the coverslip of a single 100-μm-thick section using a felt pen; 3 images were captured systematically from each area by positioning the stage within the outlined area of interest at 4× magnification before digital image capture at 20×. During image acquisition, the stage was positioned systematically within the selected areas without regard to field of view, except in cases in which large, AP-positive arteries (≥200 μm) were present in the field. For these fields, the stage was repositioned only enough to displace the larger artery. For this reason, the data on afferent vessels relate only to those smaller than 200 μm in diameter (i.e. small arteries, arterioles, and capillaries). According to the Cavalieri principle, the area fraction of a plane is equivalent to the volume fraction. Microvascular density was defined as the area fraction occupied by the vessels.

To calculate the area fraction, vessel areas (measured in pixels) were divided by the total image area (measured in pixels) and expressed as a percentage. Adobe Photoshop (Adobe Systems,

San Jose, CA) and Fovea Pro (Reindeer Games, Asheville, NC) were used to measure vascular density on digital images. The images were processed as previously described (19,20). Briefly, the pixel intensity data were filtered from color images, hue and saturation information were discarded, and the image was converted to a gray-scale. Background staining was then removed by background subtraction in which the filtered gray-scale image was duplicated and the positive vessels removed from the duplicate image with 7 repetitive iterations of a rank-opening algorithm. The number of iterations was kept constant for each image. The resulting background image was subtracted from the original gray-scale image leaving only positive vessels on the image. Algorithmic thresholding to a binary (black-and-white image) permitted measurement of the percentage of vessel density, consisting of the area occupied by the vessels (i.e. black pixels).

The main factors that influence these measurements include the depth of field and binary algorithm settings. Depth of field was controlled by collecting all digital images with the same lens and Kohler illumination settings. Using this technique for all of the cases examined, vascular densities were measured in a 3 μm-thick plane, thin enough to be considered a flat plane in a biological system. All data were analyzed using GraphPad Prism version 4 (GraphPad Software, Inc., La Jolla, CA), and R version 2.8.1 (25). A factorial mixed-design ANOVA, in which one factor is a between-subjects variable (diagnosis) and the other is a within-subjects variable (hippocampal subdivision), was used to compare the densities among the anatomic subdivisions of the hippocampus. The cutoff probability value for all tests was set at $p \leq 0.05$ for statistical significance (two-sided).

Although important data may be obtained by threshold analysis, problems arise when using different staining techniques, such as with the lead-based histochemistry used for AP labeling of afferent vessels and DAB chromogen-based immunohistochemistry used for collagen type IV labeling of total vessels. The differences in staining intensity complicate direct comparisons between afferent and total vessel density. Since the vessels are marked without need for prior image processing, these software-driven, real-time stereological methods provide a means to compare afferent and total vessels directly in MTS and non-MTS hippocampi with a minimum of disparity due to the staining method. In addition, the stereological method provides a means for systematic, random sampling in 3D space that is not subject to operator bias.

Stereological Analysis of Total and Afferent Vessel Densities (Length/Volume)

Subsequent analyses of hippocampal tissue from 6 MTS patients and 3 non-MTS controls were done using established stereological methods. The 3 controls and 1 of the MTS cases were previously measured using the binary method. Beginning with a random start, serial sections 66-μm-thick were cut from a 2-mm-thick segment of hippocampus excised at the level of the lateral geniculate nucleus. Sections were stained according to a standardized protocol such that at least 3 AP- and 3 collagen type IV-stained sections were present at 1/3 intervals. The remaining sections were used for substrate or antibody controls, immunolabeled with other antibodies or stained with H&E for structural identification.

With this protocol, the vessel density data are referenced to a 700-μm segment of the mid-hippocampus at the level of the lateral geniculate nucleus and not to the entire hippocampus. Using systematic, random sampling methods, vascular length was measured in three 1/3 spaced sections from the AP- and collagen type IV-stained series using a Microbrightfield (MBF) stereology workstation and Stereo Investigator software (Microbrightfield, Inc., Williston, VT). Stereological measures were done on a Nikon 90i combination brightfield/fluorescence microscope with automated XYZ control interfaced with Stereo Investigator. Length of afferent and total vasculature was measured using the Space Balls probe in AP- and collagen type IV-stained sections, respectively.

All analyses were done on “real time” digital images captured with a high-speed MBF color digital camera (Microbrightfield, Inc.). Contours of the 6 hippocampal subdivisions, (i.e. subiculum, CA1, CA2, CA3, CA4, and dentate gyrus) were digitally outlined on the screen image of the hippocampus visualized with a 2× objective lens. Subsequently, using a 20× objective lens (NA 0.50), a computer-generated hemispherical probe (SpaceBall) (26,27) was placed on-screen along a randomly generated grid and vascular intersections were marked using standard inclusion criteria. In 66-μm-thick sections, afferent vessel length was measured using a 50-μm hemispherical probe with the guard zone set at 3 μm. The measurement grid was set at 600 × 600 pixels. Stereo Investigator-generated planimetry data (volume and area) were calculated using the Cavalieri principle (28,29). In addition, variance due to noise, variance of systematic, random sampling and an estimated Gundersen coefficient of error (CE) for each subject and subregion were calculated. An adequate sampling fraction, which has been defined as having a CE ≤ 0.1 (28), was determined empirically for this study. The CE for each subject ranged from 0.04 to 0.08 for data from collagen type IV-stained sections and 0.04 to 0.09 for data from AP-stained sections.

Results

Neuropathologic Findings

Each case of MTS was confirmed pathologically by a board certified neuropathologist (R.T.M.). The pathologic diagnosis of MTS was based on standard criteria, including neuronal loss and gliosis in Ammon's horn and splaying of the granular neurons of the dentate gyrus. There were no additional pathologic findings in the hippocampi from the MTS group. The non-MTS hippocampi were also free of pathologic abnormalities. The hippocampal microvasculature among the MTS and non-MTS brains was evaluated in 66 μm- and 100 μm-thick celloidin-embedded tissue sections using collagen type IV immunohistochemistry and AP enzyme histochemistry. There was no obvious difference in the density of total vessels between the MTS and non-MTS groups by light microscopic examination of the collagen type IV-stained tissue sections (Fig. 1A, B). There were, however, differences in the morphology of the collagen type IV-stained vessels. In the MTS cases, numerous string vessels were identified throughout the hippocampus (Fig. 2). These 1-μm-diameter vascular structures, often present in tissues undergoing vascular remodeling or regression, label with collagen (or laminin) antibodies and have no obvious lumen or endothelial lining (23, 24). String vessels were only rarely identified in the non-MTS controls. The density of afferent vessels, as revealed by AP histochemistry, was markedly reduced in the MTS hippocampi compared to the non-MTS controls (Fig. 1C, D). This reduction was evident abruptly in area CA1, with variable degrees of loss throughout Ammon's horn. There was no obvious difference in the density of afferent vessels in the subiculum or dentate gyrus. To evaluate for the possibility of a relationship between loss of afferent vessels and loss of neurons in the MTS cases, the MTS hippocampi were examined using AP-stained tissue sections counterstained with cresyl violet acetate and light green. The degree of neuron and afferent vessel loss was scored semi-quantitatively, using a mild, moderate, and severe grading system. Each of the subareas of Ammon's horn (CA1-4) was scored separately and the results summarized in a chi-square contingency table (Table). The results indicate a strong trend toward a significant relationship between the degree of neuronal and afferent vessel loss (chi-square value 8.460; df = 4; p = 0.076).

Microvascular Density

Total and afferent vessel densities were initially evaluated quantitatively in 4 MTS cases and 3 non-MTS controls by threshold analysis. In these studies, vessel density information is represented by area fraction or the percentage of the area occupied by stained vasculature (Fig. 3). The mean density of total hippocampal vessels was 12% lower in the MTS group (3.6 ±

0.18%) in comparison to the non-MTS group (4.06 ± 0.09%); this was statistically significant ($p = 0.007$). Post-hoc testing revealed significant decreases in total vessel density in MTS hippocampal area CA2 ($p < 0.05$); in no other areas did the differences reach statistical significance (Fig. 3A). The mean density of afferent hippocampal vessels was 40% lower in the MTS group (2.30 ± 0.44%) compared to the non-MTS group (3.83 ± 0.11%) ($p < 0.0001$). While all areas except the subiculum were reduced in the MTS group, post-hoc testing revealed significant reductions only in areas CA3 ($p < 0.05$) and CA2 ($p < 0.001$) (Fig. 3B).

Results of microvascular density determinations (length/volume; mm/mm^3) in non-MTS and MTS hippocampus measured with Stereo Investigator using the Space Balls probe are shown in Figure 4. By 2-way ANOVA, the mean density of total hippocampal vessels was slightly greater in the MTS group (469.00 ± 14.56, n = 6) compared to the non-MTS group (436.96 ± 13.53, n = 3); this was not statistically significant ($p = 0.44$) (Fig. 4A). In contrast, the mean density of afferent vessels across all areas was significantly lower in the MTS hippocampi (213.73 ± 13.66) compared to non-MTS hippocampi (303.15 ± 17.39) ($p = 0.0011$) (Fig. 4B). Although a significant difference in afferent vessel density was detected collectively across all areas, post-hoc testing revealed no significant difference when comparing the individual subdivisions of the hippocampal formation. In view of the considerable atrophy in some areas of the MTS hippocampi, increases in vascular density due to packing would be expected and indeed were observed in some MTS hippocampal areas (Fig. 4A). Since the AP- and collagen type IV-labeled sections used for measurement were adjacent, any brain volume changes should be consistent for both the AP-labeled afferent and collagen-labeled total vessel densities. Therefore, a calculation of the ratio of afferent to total vessel density effectively factors out changes in area size and provides a more accurate estimate of the afferent microvascular density (Fig. 4C). Afferent vessels comprised 72.7% ± 0.04% of the total vessels in the non-MTS hippocampi and 47.5% ± 0.04% of total vessels in MTS hippocampi ($p = 0.001$). Post-hoc testing demonstrated a significant reduction only in area CA3 ($p < 0.05$).

Vessel Density and Age

Since MTS typically presents in young patients there is an age-related selection bias of hippocampal specimens that is a confounding factor; this is difficult to control because of the paucity of normal temporal lobe tissues from young individuals. The mean ages of the MTS patients (34.8 ± 7.0 years) and non-MTS patients (61.7 ± 3.0 years) were significantly different ($p = 0.037$). Therefore, to exclude age as a possible explanation for the observed reduction in afferent vessels in MTS, the density of afferent vessels was evaluated as a function of age separately within the MTS and control groups using linear regression analysis. There was no statistically significant association between the afferent microvascular density and age within the MTS or non-MTS groups in either the binary or stereological data sets.

Discussion

We investigated the hippocampi in MTS patients and non-MTS controls using thick celloidin sections, which allows for greatly enhanced visualization of the microvasculature, particularly in combination with collagen type IV and AP staining. Collagen type IV is a non-fibrillar form of collagen that plays an important role in the formation and structural integrity of basement membranes, including those of blood vessels; it has been used to study microvascular density and damage in brains from humans and in animal models (30–36). AP is thought to play an important role in the formation of the BBB (37–39); it is expressed in brain endothelial cells from afferent vessels (i.e. arterioles and capillaries), but not venules (19,22,39–43). Using image threshold and stereological methods, we found novel alterations of the hippocampal microvasculature in patients with pathologically confirmed MTS.

In some MTS hippocampal areas, we observed a slight, but not statistically significant, increase in vessel density as measured by area fraction (i.e. a reflection of both the diameter and length of vasculature), but the overall density of total vessels was found to be decreased using this methodology, primarily due to a significant decrease in total vessel density in CA2. Focal, slight increases in the total vessel density in the MTS hippocampi were also seen using stereological methods but these did not reach statistical significance. The latter methodology is not only more robust but also examines a larger area of the hippocampus, and is thus more likely to be an accurate reflection of the total vessel density in MTS hippocampi.

When afferent vessel density was evaluated in AP-stained thick sections by both image threshold and stereological methods, we found a significant reduction in the density of hippocampal afferent vessels. Morphologic comparisons revealed a marked reduction in AP-labeled afferent vessels, distinctly in area CA1 and continuing to various degrees throughout Ammon's horn with no obvious differences in the subiculum or dentate gyrus. These observations were supported by the quantitative studies. The reduction in afferent vessels reached statistical significance in areas CA2 and CA3 using the image threshold method. Using both methods, there was a strong trend toward significance in areas CA1 and CA4. When density changes due to atrophy were factored out, the ratio of afferent to total vessels reached statistical significance in area CA3. To exclude differences in age as a possible explanation for the observed reduction in afferent vascular density, we performed linear regression analysis separately within the MTS and non-MTS groups and found no statistically significant association between afferent microvascular density and age in either group. We have, however, shown in previous studies a significant age-related decline in afferent vascular density in frontal lobe tissues from normal brains (19). Importantly, such a decline in the density of afferent vessels with increasing age would only mask the differences between the younger MTS patients and the older controls in the present study.

Regardless of the actual mechanism, our data provide evidence of vascular degeneration in MTS hippocampi, including an increase in the number string vessels. These small collagenous vascular structures are typically found in regions of vascular atrophy and degeneration and are thought to represent the collagen remnants of degenerating blood vessels (23,24). The reduction in AP-labeled afferent vessels may similarly represent a degenerative phenomenon, whether by physical loss of afferent vessels or by a reduction in the activity or expression of this enzyme in degenerating vessels. The reduction in this BBB-associated enzyme in the microvasculature of Ammon's horn is consistent with recent reports of extravasation of proteins (14,15), increases in BBB permeability (15), and vascular wall alterations (16) in MTS.

Recent human and animal model studies suggest that vascular density is increased in MTS. Rigau et al examined temporal lobe tissues using very thin (4 μm) sections and demonstrated a modest increase in longitudinal profiles of small vessels in area CA1 and the dentate gyrus in the epileptic patients, including those with and without MTS (14). They also examined rat hippocampi using a pilocarpine-induced chronic epilepsy model and 30 μm thick sections and demonstrated an increase in the density of small vessels, principally in area CA1. Other animal model studies, including Hellsten et al (18) and Marcon et al (17), also suggest that the density of hippocampal microvessels increases in the setting of chronic epilepsy.

Similar to some of the animal model studies, we did find a modest increase in total vessels in the hippocampus in a subset of the patients. Averaged among all of the cases, however, this did not reach statistical significance. To the contrary, our data show a consistent reduction in the density of afferent microvessels in the MTS hippocampi, including a reduction in the ratio of afferent to total vessels. Our results appear to contradict the findings in previous studies, the strongest data of which are based on animal models. The observed discrepancies could represent a difference in tissue response between humans and rodents. Another possible

explanation, particularly when comparing the human data, is that the observed increase in total vessels may be secondary to the phenomenon of vascular packing in areas of hippocampal atrophy. We controlled for this by providing varying measures of vascular density, including a measurement of the ratio of afferent to total vessels.

Our data raise the possibility that alterations in the afferent vascular supply may play a role in the pathogenesis of MTS. Possible mechanisms include reduced perfusion and / or disruption of the blood-brain-barrier. In general, the density of afferent vessels correlates directly with the degree of tissue perfusion and local cerebral blood flow (44). Based on these observations, a pathological decrease in the density or function of afferent vessels should lead to a reduction in regional perfusion. Radiological studies of MTS patients would seem to support this hypothesis. For example, single photon emission computed tomography (SPECT) imaging in pathologically confirmed cases of MTS has demonstrated consistent interictal hypoperfusion (45). Additionally, studies using pulsed arterial spin labeling MRI have shown similar results, with hypoperfusion in the MTS hippocampus (46). In keeping with the observed hypoperfusion, fluorodeoxyglucose positron emission tomography (FDG-PET) studies show hypometabolism in the affected hippocampus in MTS (47).

In summary, we have demonstrated a significant decrease in the density of afferent vessels in MTS hippocampi. In light of previous studies, our data may reflect the complex and dynamic nature of tissue responses in the CNS. Dynamic tissue responses are well-recognized in non-CNS tissues, including in the setting of wound healing, in which there is an early hypervascular response, followed later by decreased vascularity and scarring. Our findings may have important implications in furthering our understanding of the pathogenesis and pathophysiology of MTS.

Acknowledgments

The authors gratefully acknowledge the expertise of Patricia Wood and Carolyn Cox in the preparation of histological specimens. We also thank the nurses, technicians and staff of the Neurosurgical Unit of Wake Forest University Baptist Hospital for their help.

This work was supported by NIH grants NS020618 and CA113321.

References

1. Cavanagh JB, Meyer A. Aetiological aspects of Ammon's horn sclerosis associated with temporal lobe epilepsy. Br Med J 1956;2:1403–7. [PubMed: 13374345]
2. Meyer A, Falconer MA, Beck E. Pathological findings in temporal lobe epilepsy. J Neurol Neurosurg Psychiatry 1954;17:276–85. [PubMed: 13212417]
3. Meyer A, Beck E. The hippocampal formation in temporal lobe epilepsy. Proc R Soc Med 1955;48:457–62. [PubMed: 14395254]
4. Thom M. Hippocampal sclerosis: progress since Sommer. Brain Pathol. 2008Epub ahead of print Published Online: 29 Aug 2008
5. Meiners LC, van GA, Jansen GH, et al. Temporal lobe epilepsy: The various MR appearances of histologically proven mesial temporal sclerosis. AJNR Am J Neuroradiol 1994;15:1547–55. [PubMed: 7985576]
6. Sommer W. Erkrankung des ammonshorns ala aetiologioches moment der epilepsien. Arch Psychiatr Nervenkr 1880;10:631–75.
7. Spielmeyer W. Die pathogenese des epileptisches krampfes, histopathologischer teil. Ztschr Neurol Psychiat 1927;109:501–19.
8. Houser CR. Granule cell dispersion in the dentate gyrus of humans with temporal lobe epilepsy. Brain Res 1990;535:195–204. [PubMed: 1705855]

9. Bouchet C, Cazauvieil H. De l'epilepsie consideree dans ses rapports avec l'alienation mentale: Recherche sur la nature et le siege de ces deux maladies. Arch Gen Med 1825;9:510–42.
10. Bratz E. Ammonshornbefunde bei epileptikern. Arch Psychiatr Nervenkr 1899;32:820–35.
11. Cendes F, Andermann F, Dubeau F, et al. Early childhood prolonged febrile convulsions, atrophy and sclerosis of mesial structures, and temporal lobe epilepsy: an MRI volumetric study. Neurology 1993;43:1083–87. [PubMed: 8170546]
12. Harvey AS, Grattan-Smith JD, Desmond PM, et al. Febrile seizures and hippocampal sclerosis: Frequent and related findings in intractable temporal lobe epilepsy of childhood. Pediatr Neurol 1995;12:201–6. [PubMed: 7619185]
13. Waruiru C, Appleton R. Febrile seizures: An update. Arch Dis Child 2004;89:751–56. [PubMed: 15269077]
14. Rigau V, Morin M, Rousset MC, et al. Angiogenesis is associated with blood-brain barrier permeability in temporal lobe epilepsy. Brain 2007;130:1942–56. [PubMed: 17533168]
15. van Vliet EA, da Costa AS, Redeker S, et al. Blood-brain barrier leakage may lead to progression of temporal lobe epilepsy. Brain 2007;130:521–34. [PubMed: 17124188]
16. Hildebrandt M, Amann K, Schroder R, et al. White matter angiopathy is common in pediatric patients with intractable focal epilepsies. Epilepsia 2008;49:804–15. [PubMed: 18266747]
17. Marcon J, Gagliardi B, Balosso S, et al. Age-dependent vascular changes induced by status epilepticus in rat forebrain: Implications for epileptogenesis. Neurobiol Dis 2009;34:121–32. [PubMed: 19320047]
18. Hellsten J, West MJ, Arvidsson A, et al. Electroconvulsive seizures induce angiogenesis in adult rat hippocampus. Biol Psychiatry 2005;58:871–78. [PubMed: 16043138]
19. Moody DM, Thore CR, Anstrom JA, et al. Quantification of afferent vessels shows reduced brain vascular density in subjects with leukoaraiosis. Radiology 2004;233:883–90. [PubMed: 15564412]
20. Anstrom JA, Brown WR, Moody DM, et al. Temporal expression pattern of cerebrovascular endothelial cell alkaline phosphatase during human gestation. J Neuropathol Exp Neurol 2002;61:76–84. [PubMed: 11829346]
21. Anstrom JA, Thore CR, Moody DM, et al. Morphometric assessment of collagen accumulation in germinal matrix vessels of premature human neonates. Neuropathol Appl Neurobiol 2005;31:181–90. [PubMed: 15771711]
22. Bell MA, Scarrow WG. Staining for microvascular alkaline phosphatase in thick celloidin sections of nervous tissue: Morphometric and pathological applications. Microvasc Res 1984;27:189–203. [PubMed: 6369077]
23. Challa VR, Thore CR, Moody DM, et al. A three-dimensional study of brain string vessels using celloidin sections stained with anti-collagen antibodies. J Neurol Sci 2002:203–204. 165–67.
24. Challa VR, Thore CR, Moody DM, et al. Increase of white matter string vessels in Alzheimer's disease. J Alzheimer's Dis 2004;6:379–83. [PubMed: 15345807]
25. R Development Core Team R: A Language and Environment for Statistical Computing. Vienna, Austria: R Foundation for Statistical Computing; 2008.
26. Kubinova L, Janacek J. Confocal microscopy and stereology: Estimating volume, number, surface area and length by virtual test probes applied to three-dimensional images. Microsc Res Tech 2001;53:425–35. [PubMed: 11525261]
27. Mouton PR, Gokhale AM, Ward NL, West MJ. Stereological length estimation using spherical probes. J Microsc 2002;206:54–64. [PubMed: 12000563]
28. Gundersen HJ, Jensen EB. The efficiency of systematic sampling in stereology and its prediction. J Microsc 1987;147:229–63. [PubMed: 3430576]
29. Gundersen HJ. Stereology of arbitrary particles. A review of unbiased number and size estimators and the presentation of some new ones, in memory of William R. Thompson. J Microsc 1986;143:3–45. [PubMed: 3761363]
30. Buttner A, Kroehling C, Mall G, et al. Alterations of the vascular basal lamina in the cerebral cortex in drug abuse: A combined morphometric and immunohistochemical investigation. Drug Alcohol Depend 2005;79:63–70. [PubMed: 15943945]

31. Grobholz K, Burggraf D, Martens KH, et al. Recombinant tissue plasminogen activator attenuates basal lamina antigen loss after experimental focal cerebral ischemia. Neurol Res 2005;27:212–17. [PubMed: 15829186]
32. Hamann GF, Liebetrau M, Martens H, et al. Microvascular basal lamina injury after experimental focal cerebral ischemia and reperfusion in the rat. J Cereb Blood Flow Metab 2002;22:526–33. [PubMed: 11973425]
33. Hamann GF, Schrock H, Burggraf D, et al. Microvascular basal lamina damage after embolic stroke in the rat: relationship to cerebral blood flow. J Cereb Blood Flow Metab 2003;23:1293–97. [PubMed: 14600436]
34. Liebetrau M, Burggraf D, Buscher C, et al. Ramipril prevents extracellular matrix accumulation in cerebral microvessels. Neurol Res 2005;27:477–82. [PubMed: 16025600]
35. Uspenskaia O, Liebetrau M, Herms J, et al. Aging is associated with increased collagen type IV accumulation in the basal lamina of human cerebral microvessels. BMC Neurosci 2004;5:37. [PubMed: 15387892]
36. Vosko MR, Burggraf D, Liebetrau M, et al. Influence of the duration of ischemia and reperfusion on infarct volume and microvascular damage in mice. Neurol Res 2006;28:200–205. [PubMed: 16551441]
37. Calhau C, Martel F, Pinheiro-Silva S, et al. Modulation of insulin transport in rat brain microvessel endothelial cells by an ecto-phosphatase activity. J Cell Biochem 2002;84:389–400. [PubMed: 11787068]
38. Meyer J, Mischeck U, Veyhl M, et al. Blood-brain barrier characteristic enzymatic properties in cultured brain capillary endothelial cells. Brain Res 1990;514:305–9. [PubMed: 1972640]
39. Vorbrodt AW, Lossinsky AS, Wisniewski HM. Localization of alkaline phosphatase activity in endothelia of developing and mature mouse blood-brain barrier. Dev Neurosci 1986;8:1–13. [PubMed: 3743466]
40. Jefferys JG. Influence of electric fields on the excitability of granule cells in guinea-pig hippocampal slices. J Physiol 1981;319:143–52. [PubMed: 7320909]
41. Moody DM, Brown WR, Challa VR, et al. Cerebral microvascular alterations in aging, leukoaraiosis, and Alzheimer's disease. Ann N Y Acad Sci 1997;826:103–16. [PubMed: 9329684]
42. Thore CR, Anstrom JA, Moody DM, et al. Morphometric analysis of arteriolar tortuosity in human cerebral white matter of preterm, young, and aged subjects. J Neuropathol Exp Neurol 2007;66:337–45. [PubMed: 17483690]
43. Ushiki T, Abe K. Identification of arterial and venous segments of blood vessels using alkaline phosphatase staining of ink/gelatin injected tissues. Arch Histol Cytol 1998;61:215–19. [PubMed: 9756098]
44. Gjedde A, Diemer NH. Double-tracer study of the fine regional blood-brain glucose transfer in the rat by computer-assisted autoradiography. J Cereb Blood Flow Metab 1985;5:282–89. [PubMed: 3988827]
45. Hartley LM, Gordon I, Harkness W, et al. Correlation of SPECT with pathology and seizure outcome in children undergoing epilepsy surgery. Dev Med Child Neurol 2002;44:676–80. [PubMed: 12418792]
46. Lim YM, Cho YW, Shamim S, et al. Usefulness of pulsed arterial spin labeling MR imaging in mesial temporal lobe epilepsy. Epilepsy Res 2008;82:183–89. [PubMed: 19041041]
47. Boling WW, Lancaster M, Kraszpulski M, et al. Fluorodeoxyglucose-positron emission tomographic imaging for the diagnosis of mesial temporal lobe epilepsy. Neurosurgery 2008;63:1130–38. [PubMed: 19057325]

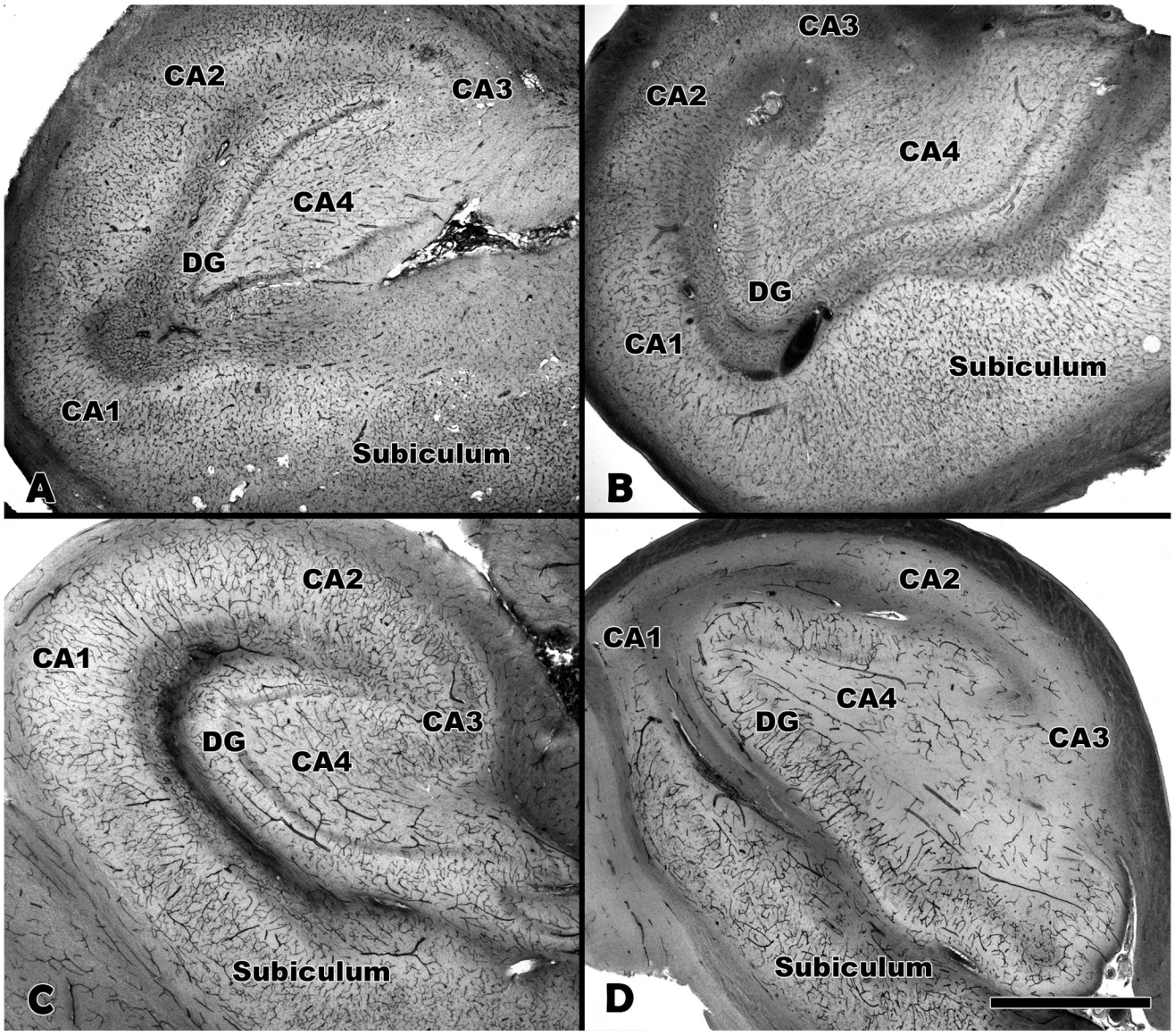

Figure 1.

Collagen type IV and alkaline phosphatase (AP) staining of hippocampi. (**A, B**) Total vasculature is labeled with antibody to collagen type IV. (**C, D**) Afferent vessels labeled by alkaline phosphatase histochemistry. Control hippocampus (**A, C**) and MTS hippocampus (**B, D**) are shown at 2× magnification. The density of afferent vessels (**D**) is markedly reduced in the MTS hippocampus compared to the control hippocampus (**C**). MTS, mesial temporal sclerosis; DG, dentate gyrus; CA, cornu Ammons. Bar = 1 mm.

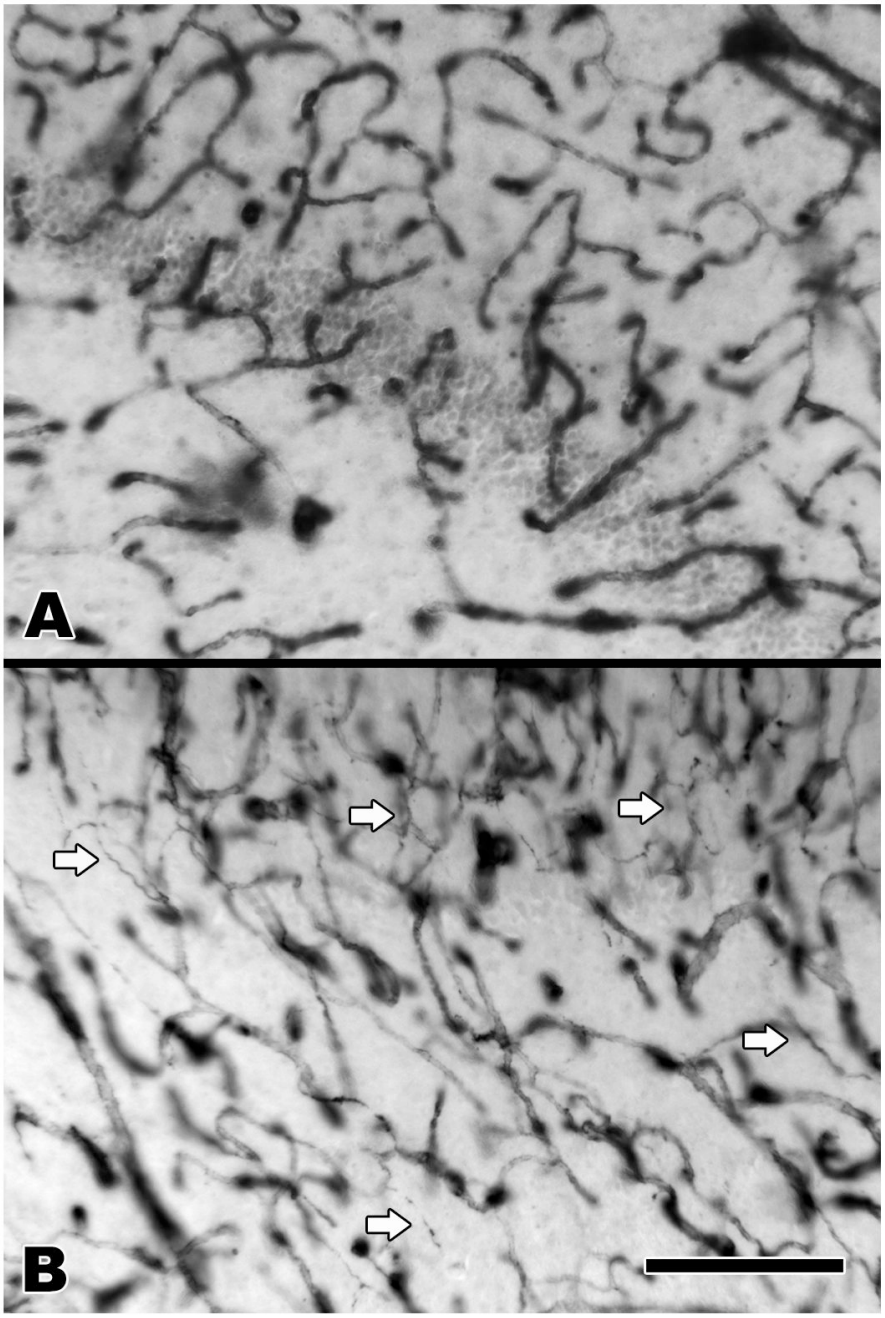

Figure 2.
Dentate gyrus and CA4 stained with collagen type IV antibody. (**A**) Non-MTS, (**B**) MTS. Multiple string vessels that indicate areas of regressing vasculature are seen in the MTS hippocampus (arrows). CA4, cornu Ammons area 4; MTS, mesial temporal sclerosis. Bar = 200 μm.

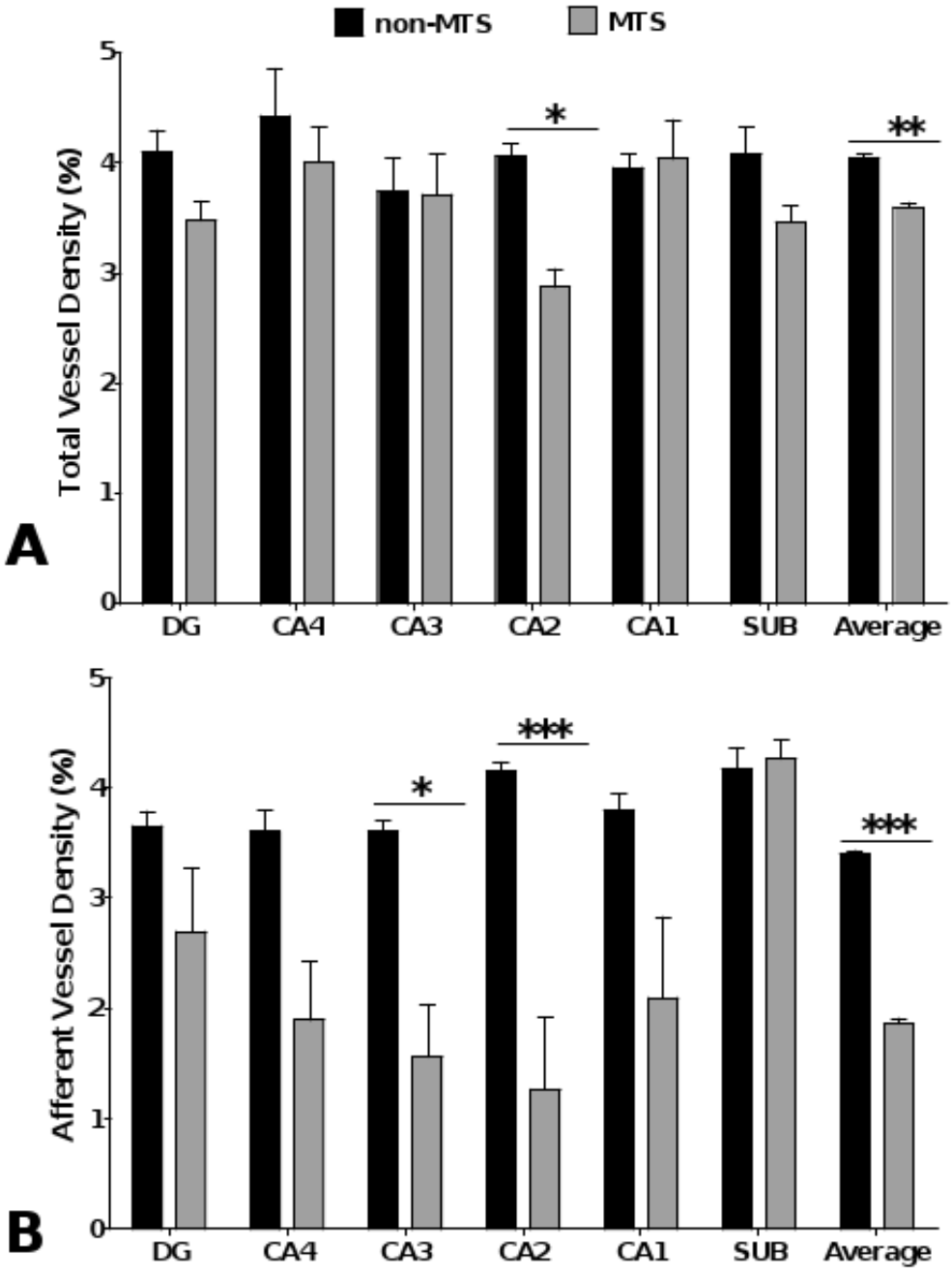

Figure 3.

Bar graph illustrating vessel density measured as area fraction. ANOVA analysis confirmed that overall total vessel density (**A**) was significantly decreased in MTS ($p = 0.007$) with significant differences in area CA2 ($p < 0.05$). Afferent vessel density (**B**) was significantly decreased ($p < 0.001$) in MTS with significant differences in the areas CA3 ($p < 0.05$) and CA2 ($p < 0.001$). MTS, mesial temporal sclerosis; CA2, cornu ammons area 2; CA3, cornu Ammons area 3.

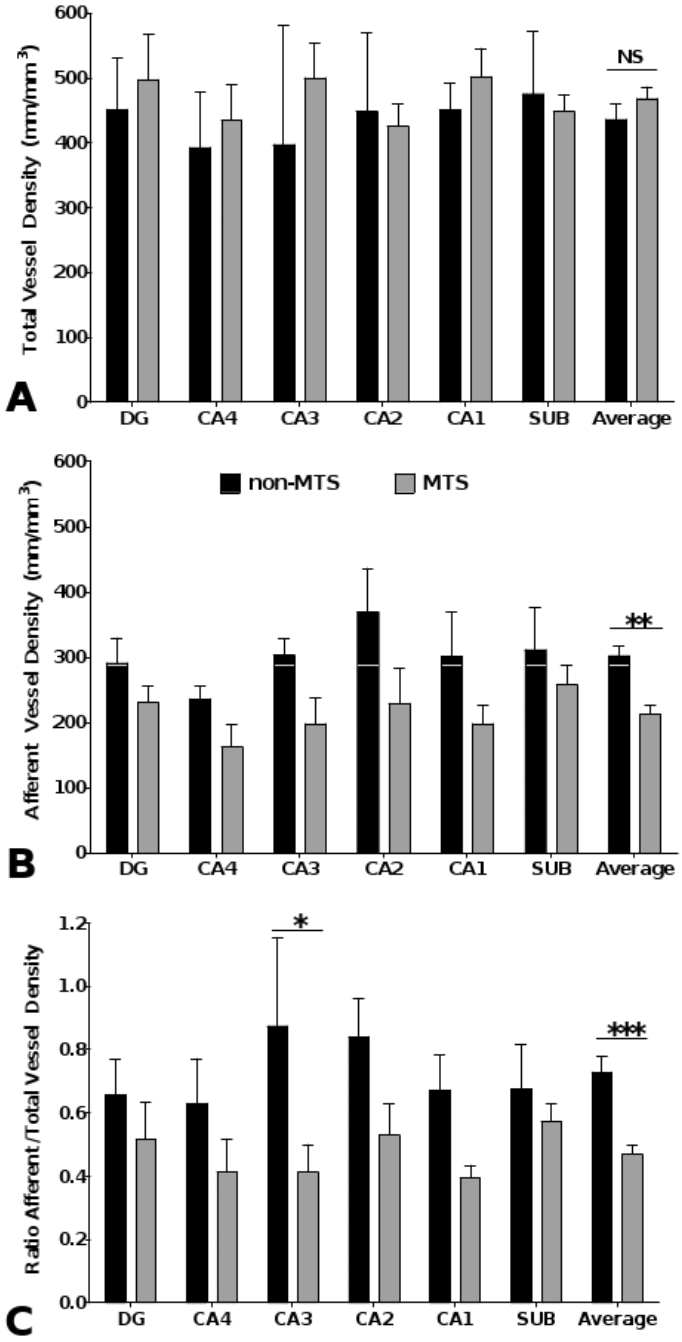

Figure 4.

Bar graph illustrating vessel density as length/volume (mm/mm^3) assessed by stereological methods. Statistical analysis by 2-way ANOVA revealed that total vessel density (**A**) was not significantly different between the non-MTS and MTS groups. MTS afferent vessel density (**B**) and the ratio of afferent/total vessels (**C**) were both decreased significantly ($p = 0.001$ for both). MTS, mesial temporal sclerosis.

Table

Chi Square Table Summarizing Frequency Distributions of Neuron and Afferent Vascular Loss In Medial Temporal Sclerosis Hippocampus Cases

		Neuron Loss			
		Mild	**Moderate**	**Severe**	**Afferent vessel Total**
Afferent vessel loss	Mild	8	3	0	11
	Moderate	5	6	3	14
	Severe	1	3	3	7
	Neuron Total	14	12	6	32

Neuron and afferent vessel loss were categorized as mild, moderate, or severe.